Carbohydrate Polymers 87 (2012) 435–443

Contents lists available at ScienceDirect

Carbohydrate Polymers

journal homepage: www.elsevier.com/locate/carbpol

Biocomposite films prepared from ionic liquid solutions of chitosan and cellulose

Cristina Stefanescu[a,*], William H. Daly[a], Ioan I. Negulescu[a,b]

[a] Department of Chemistry, Louisiana State University, Baton Rouge, LA 70803, USA
[b] School of Human Ecology and LSU Agricultural Center, Louisiana State University, Baton Rouge, LA 70803, USA

ARTICLE INFO

Article history:
Received 7 June 2011
Received in revised form 25 July 2011
Accepted 1 August 2011
Available online 9 August 2011

Keywords:
Chitosan
Cellulose
Ionic liquid
Blends

ABSTRACT

Blends of chitosan and cellulose were successfully produced using 1-butyl-3-methylimidazolium acetate (BMIMAc) as solvent media. Films were prepared from the blends by manually spreading the solution on a flat surface and precipitating the polymers in a mixture of methanol and water. To prevent the shrinkage of films, most of the absorbed water was removed by freeze drying under vacuum. Films prepared from the polymeric solutions were investigated by means of FT-IR, TGA, X-ray diffraction and SEM measurements. The shifting of the bands corresponding to –NH and C=O groups of chitosan (FT-IR), the absence of the diffraction peaks at $2\theta = 10.7$ and 14.9° (XRD), the increased E_a for thermal decomposition for all the polymeric blends (MTGA), and the presence of an apparent homogeneous structure with no phase separation of the two polymers (SEM) provide evidence for the miscibility between chitosan and cellulose in the solid state.

1. Introduction

Chitosan, a linear β-linked polysaccharide and natural biopolymer, has been widely studied due to its extensive applications in chemical, biochemical and biomedical fields. Chemically, chitosan is composed of randomly distributed β-(1-4)-linked deacetylated D-glucosamine units and N-acetyl-D-glucosamine units. Because of its high density of amino groups chitosan has very good coagulating properties, acting as a flocculant/coagulant in the presence of negatively charged polymers, proteins, dyes, etc. (Goosen, 1997; Muzzarelli, 1973). It is generally insoluble in organic solvents, water and alkaline solutions (Goosen, 1997). The polysaccharide dissolves in solutions of nearly all organic acids at pH values below 6 where chitosan behaves as a cationic polymer. Perhaps the most frequently used organic acids to prepare chitosan solutions are acetic acid and formic acid. In addition, several dilute inorganic acid solutions (e.g. HNO_3, H_3PO_4, HCl, and $HClO_4$) can be employed to dissolve chitosan.

Among the many reasons behind the continuous search for new applications of chitosan are the polymer's biodegradability, non-toxicity and natural abundance. Chitosan possesses film forming characteristics, but the physical properties of fabricated products are not very satisfactory. Chitosan containing membranes and gels have been employed over the years in water purification, filtration, fruit coating, surgical dressings and drug encapsulation (Nakajima & Shinoda, 1977; Rha, Rodriguez-Sanchez, & Kienzle-Sterzer, 1984; Shigehiro, Kenji, Masahiro, & Noriaki, 1980; Wu, Bough, Holmes, & Perkins, 1978). Further application for chitosan are found in paper-making, food processing, pharmaceutics and biotechnology. Positive contributions to these applications are attributable to chitosan's ability to accelerate wound healing and plant germination and to stimulate the immune system. Therefore, incorporating chitosan into polymer blends is frequently used to obtain new materials with antimicrobial properties and better thermal stability. The thermal stability of the blends depends strongly on the compatibility of the polymers (Rao & Johns, 2008).

Blending of polymers to improve their chemical and physical properties has been received substantial attention in the past years (Flores-Ramirez et al., 2005; Luo, Yin, Khutoryanskaya, & Khutoryanskiy, 2008; Pawlak & Mucha, 2003; Wu et al., 2004; Xu, Kim, Hanna, & Nag, 2005; Yin, Luo, Cheng, & Khutoryanskiy, 2006; Zhao et al., 2009). In a common solvent, polymer mixtures may form homogeneous solutions. Fibers or films obtained from homogeneous solutions of two mixed polymers have unique physical properties as well as other characteristics of both polymeric components. Chitosan and cellulose are renewable, biodegradable, and biocompatible polymers, but difficult to process by dissolving into common solvents. This is due to the presence of intra and intermolecular hydrogen bonding and molecular close chain packing. Almeida et al. prepared chitosan/cellulose biocomposite films using NaOH/thiourea as solvent (Almeida, Frollini, Castellan, & Coma, 2010). The dissolution process is accompanied by depolymerization of both polymers and some deacetylation of chitosan. Wu et al. prepared polysaccharides-based membranes of chitosan and cellulose blends using trifluoroacetic acid as a co-solvent (Wu

---

[*] Corresponding author. Tel.: +1 225 578 1684; fax: +1 225 578 3458.
E-mail addresses: cmart56@lsu.edu, cristinastefanescu@alumni.lsu.edu (C. Stefanescu).

0144-8617/$ – see front matter © 2011 Elsevier Ltd. All rights reserved.
doi:10.1016/j.carbpol.2011.08.003

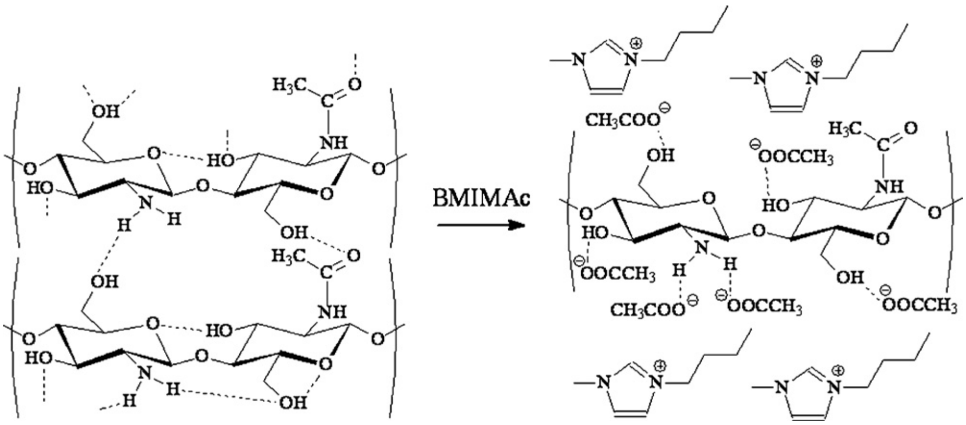

Scheme 1. Dissolution of chitosan in 1-butyl-3-methylimidozolium acetate (BMIMAc).

et al., 2004). The results indicated that the cellulose/chitosan blends were not well miscible. Phisalaphong et al. prepared films of chitosan and bacterial cellulose by means of adding 0.25–0.75% (w/v) of low-molecular-weight chitosan in the culture medium during biosynthesis by *Acetobacto xylinum* (Phisalaphong & Jatupaiboon, 2008). The films were homogeneous and the intermolecular interaction between the hydroxyl groups of cellulose and the amino groups of chitosan were indicated by FT-IR spectra. The mechanical properties and the water absorption capacity of films were significantly improved but no significant influence on some properties of the films such as water vapor transmission rates, average crystallinity index and anti-microbial ability were observed with the addition of chitosan of low-molecular-weight in the dilute concentration. Simmon et al. reported that 0.5 wt% chitosan can be added to cellulose, xylan and lignin blends to produce a synthetic wood composite films with potential antibacterial properties (Simmons et al., 2010). Cellulose/chitosan blend films have been cast from N-methylmorpnholine-N-oxide (NMMO) to yield homogeneous biostatic films with chitosan concentrations less than 6 wt% (Shih, Shieh, & Twu, 2009). A blend 1:2 low molecular weight chitosan/cellulose prepared by codissolution of the components in BMIMCl yielded effective biosorbant foams for heavy metal ion adsorption (Sun, Peng, Ji, Chen, & Li, 2009). Recently, Xiao et al. employed a binary ionic liquid solvent (1,3-dimethylimidazoium chloride and 1-H-3-methylimidizolium chloride) to produce 3:1 cellulose/chitosan blended membranes (Xiao, Chen, Wu, & Wu, 2011).

Ionic liquids have been found particularly useful in dissolution of polar organic materials, even polymers, which are otherwise difficult to dissolve (Rogers & Seddon, 2003). Ionic liquids, organic salts with melting points under100 °C, are of great interest due to their lack of vapor pressure over a wide range of temperature, high thermal stability, non-flammability, environmental compatibility, and tunable solubility properties (Rogers & Seddon, 2003). Ionic liquids are able to dissolve chitosan (Stefanescu, Daly, & Negulescu, 2009a, 2009b) and cellulose (Liu et al., 2007a; Liu, Sun, Zhang, & Ren, 2007b; Swatloski, Spear, Holbrey, & Rogers, 2002; Zhu et al., 2006) under suitable conditions by completely disrupting the hydrogen bonds existent in their structure. The proposed action of the ionic liquid, 1-butyl-3-methylimidozolium acetate (BMIMAc) is illustrated in Scheme 1.

The present investigation reports the formation of chitosan–cellulose blends in BMIMAc and preparation of porous films from the corresponding polymeric solutions. Since the molecular structure of chitosan and cellulose are very similar, it is expected that the blend films to have high compatibility and miscibility. Our interest in obtaining films from blends of chitosan and cellulose is owed to skin tissue regeneration and accelerate healing of wounds effect created by the presence of chitosan that has distinctive biomedical properties when used as wound-dressing materials.

Sun et al. reported the dissolution of both chitosan and cellulose in BMIMCl (Sun et al., 2009). However, high molecular weight chitosan with a Brookfield viscosity of 200,000 cps will only swell in BMIMCl (Stefanescu et al., 2009b). A complete dissolution of chitosan could not be observed when heating at 100 °C not even after 4 days. In contrast, BMIMAc is capable of dissolving the entire molecular weight range of chitosan. We wish to report the preparation of chitosan/cellulose porous films with chitosan contents ranging from 5 to 50 wt% using BMIMAc as the solvent. The physical properties of the polymeric films cast from the blend solutions and dried by lyophilization will be discussed.

2. Experimental

2.1. Materials

All chemicals were used as received from the vendors. 1-Butyl-3-methylimidazolium acetate (BMIMAc) and chitosan, with a Brookfield viscosity of 200,000 cps (1% solution in 1% acetic acid) were purchased from Sigma Aldrich Chemical Company. The cellulose used, pulp powder with a degree of polymerization of 670, was a gift from Buckeye Tech. Inc. (Memphis, TN). Both chitosan and cellulose were dried over night at 90 °C and used without any further purification.

2.2. Preparation of biocomposite films

The dissolution of chitosan or cellulose in the 1-butyl-3-methylimidazolium acetate (BMIMAc) ionic liquid was performed by adding the polysaccharide to BMIMAc in a vial under argon followed by heating the slurry to 85–95 °C and agitating with an overhead mixer. The dissolution time varied with the weight percentage and the type of polymer added to the ionic liquid. The dissolution time allotted for a 6 wt% chitosan was about 3–4 days while the time for the corresponding weight percent cellulose was 12 h. Six distinct solutions were prepared using chitosan and/or cellulose with a total concentration of 6 wt%. Two solutions were made of either neat chitosan or neat cellulose, while the other four solutions were blends of the neat solutions with chitosan-to-cellulose weight percent ratios of 5/95, 10/90, 25/75, and 50/50, respectively. The blends were obtained by mixing the cellulose and chitosan solutions in a glove box to prevent the exposure to moisture. Next, the blend solutions were mixed manually under

Table 1
FT-IR absorption of polymeric blends (chitosan–cellulose).

	Chitosan	Chitosan/cellulose 5/95	Chitosan/cellulose 10/90	Chitosan/cellulose 25/75	Chitosan/cellulose 50/50	Cellulose
A	3430	3434	3436	3427	3428	3430
B	2919	2920	2920	2920	2919	2919
C	1659	1637	1629	1640	1643	1637
D	1597	–	–	1565	1565	–
E	1422	1425	1425	1425	1422	1422
F	1378	1375	1377	1377	1378	1374
G	1154	1158	1159	1157	1156	1158
H	1072	1067	1067	1069	1069	1067

Where A: –OH and –NH stretching; B: –CH stretching; C: C=O stretching (amide I), and absorbed water in the amorphous region; D: –NH bending (amide II); E: –CH and –NH bending vibrations; F: $-CH_3$ bending vibrations; G: Anti-symmetric stretching of the C–O–C bridge; H: Skeletal vibrations involving the C–O stretching.

argon with a spatula every 4–6 h for 2 days. Between the mixing processes the vials were kept in an oven at 50 °C. All solutions, containing chitosan–cellulose blends, cellulose or chitosan are clear and transparent as opposed to the polymeric-BMIMAc slurries prior to dissolution. Films were prepared from each composition by manually spreading the solutions on a flat Teflon surface with a glass rod. The thickness of the spreading was kept constant at 1.5 mm. Following the spreading of solutions, the Teflon surface was dipped into a mixture of methanol and water (50–50 by vol.) to precipitate the films. The crude films were washed several times with methanol and water and finally just with distilled water. In order to prevent the shrinkage of films, most of the absorbed water was removed by freeze drying under vacuum. A Labconco Freeze Dryer was used to freeze dry the wet polymeric films after they were previously frozen using liquid nitrogen. A high vacuum (0.010 mBar) and a temperature of −89 °C were employed during the drying process. The samples were allowed to rest at these conditions for 24 h. Finally the films were stored in desiccators to remove any residual traces of water.

2.3. *Characterization methods*

2.3.1. *Infrared analysis*

FT-IR spectra of the freeze-dried polymeric blends were recorded on a ThermoNicolet 300 Fourier Transform Infrared spectrometer using a KBr disc containing 1% of very fine ground samples. One hundred scans were taken for each sample in the range of 4000–400 cm^{-1} at a resolution of 4 cm^{-1} in the transmission mode.

The degree of acetylation of chitosan (15%) was determined by using the method of Miya, Iwamoto, Yoshikawa, and Mima (1980). The following formula was used for the calculation of the % of acetyl content: $(A_{1647}\,cm^{-1}/A_{3435}\,cm^{-1})100/1.33$, where the $A_{3435}\,cm^{-1}$ of the –OH band was used as a reference. The areas were calculated after drawing a baseline for the pertinent absorbances.

2.3.2. *Thermogravimetric analysis (TGA)*

Thermogravimetric analysis (TGA) of polymeric film samples (∼2 mg) was performed on a TA Instruments TGA 2950 thermobalance under nitrogen. The polymeric films were previously dried at 50 °C before executing the analysis. For isothermal degradation analysis the samples were heated from ambient temperature to 200 °C with a heating rate of 10 °C min^{-1} and held in isothermal mode at this temperature for 5 h. The polymeric films were previously dried at 50 °C before performing the TGA analyses.

The modulated thermogravimetric analysis (MTGA) developed by TA Instruments was carried out in order to obtain kinetic parameters during a mass loss (MTGA, xxxx). An oscillatory temperature program was used to this aim in the present study as follows: (1) high resolution sensitivity 1; (2) modulate ±5 °C every 200 s; and (3) ramp 2.00 °C min^{-1} to 600 °C with resolution 4.

2.3.3. *Scanning electron microscopy (SEM)*

Scanning electron microscopy (SEM) measurements were made using a Hitachi S-3600N microscope with a voltage of 15 kV. Prior to SEM measurements the samples were freeze-fractured in order to expose the edge of the film and sputter-coated with a thin layer of gold.

2.3.4. *X-ray diffraction measurements*

The X-ray diffraction measurements of sample foams were made using a Siemens-Bruker D5000 X-ray diffractometer with a Cu K_α radiation of 1.54 Å. Diffraction patterns were collected from $2\theta = 2$–35° with steps of 0.02° and a scan time of 2 s per step. Samples were dried at 50 °C before each measurement. Powdered samples of cellulose and chitosan were examined as reference materials. All collected data were normalized to the same baseline and shifted along the intensity axis for a better comparison of final results.

3. Results and discussion

3.1. *FT-IR analysis of polymeric films*

Formation of homogeneous chitosan and cellulose blends can be attributed to strong interactions via hydrogen bonds between the functional groups of the blend components. FT-IR spectroscopy was used to examine these interactions between chitosan and cellulose. The results of the FT-IR spectra of the chitosan–cellulose blends are presented in Table 1 and Fig. 1. It can be seen that the characteristic bands of chitosan and cellulose are present in the spectra of their blends. The spectrum of cellulose film shows similar bands to that of chitosan film except for the absorption band at 1597 cm^{-1} (Table 1) which is characteristic to –NH bending in amides and amines present in the chitosan structure. The absorption band of chitosan at 1659 cm^{-1} corresponds to carbonyl stretch in amides. The shifting of the carbonyl band to a lower frequency (1643 or 1640 cm^{-1}) suggests that these groups are involved in H-bonding with the cellulose functional groups. The presence of only one peak for the blends containing 5 wt% and 10 wt% chitosan with its value shifted to a lower frequency is indicative of interactions between the two polymers. The –NH bending in amides and amines is no longer observed in the spectra of these 2 polymeric films because the band was shifted to a higher frequency overlapping with the carbonyl stretch in amides. This shifting to a higher frequency indicates that the –NH groups of chitosan are involved in hydrogen bonding with the functional groups of cellulose, leading to a good miscible film (Luo et al., 2008). Xu and coworkers had reported a similar shift of the amino-group band of chitosan from 1578 cm^{-1} to 1584 cm^{-1} in the composite films with starch, a shift which the authors attributed to the interaction between the component polymers confirming their molecular miscibility (Xu et al., 2005). Note that no bands around 1730 cm^{-1} are observed. This band would be present if

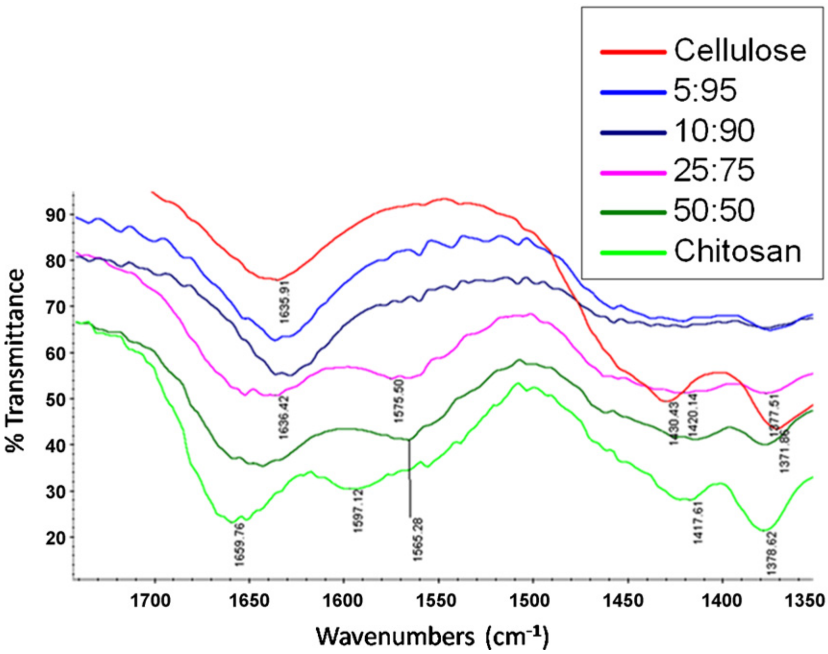

Fig. 1. FT-IR spectra of cast films of cellulose, chitosan, and chitosan–cellulose blends.

acetylation of the polysaccharides occurred due to presence of the acetate counterion in the BMIMAc solvent.

3.2. TGA analysis of polymeric films

The thermal degradation of chitosan film consisted of a thermal event that started at 251 °C with the maximum rate at 268 °C which was related to the scission of chitosan backbone. The thermal degradation of cellulose was observed at 303 °C with a maximal rate at 328 °C. As indicated by derivative traces (DTG) plotted in Fig. 2, the maximum decomposition rates were recorded at 324 °C for the samples made of chitosan–cellulose 5/95% (w/w) and 10/90%. The DTG degradation profiles of the films cast from solutions containing chitosan–cellulose 5/95% and 10/90% (w/w) displayed only one peak that has an intermediate value between that of the peaks corresponding to chitosan and cellulose, respectively. The presence of one maximum rate of degradation (mono-modal peak) for these blends, with the DTG peak shifted to a lower temperature as compared to the peak temperature of neat cellulose, is indicative of certain interactions established between the two polymers. However, in the case of chitosan–cellulose 25/75% and 50/50% (w/w) films, two maximum rates of degradation at 273 °C and 322 °C for chitosan–cellulose 25/75%, and 270 °C and 316 °C for the corresponding 50/50% blend were observed. Neither of these values matches the temperatures of peak decomposition rates of neat polymers, being slightly shifted from the peak temperatures recorded for the pure polymers. This behavior may be explained by a complementary interaction between chitosan and cellulose that impacted the decomposition temperature of each component. TGA analyses for physical mixtures of the two polymers, chitosan and cellulose, were also performed (Fig. 3). The thermogram of a 10/90% chitosan–cellulose physical mixture exhibited two maximum peaks of degradation, as opposed to only one peak observed in the thermal degradation traces of the homogeneous 10/90% chitosan–cellulose film. The thermal stability of the chitosan–cellulose blends at 350 °C was intermediate between that of pure chitosan and pure cellulose samples. It can be observed that the higher content of chitosan enhances the char yield of the blends (Fig. 4). Thus, the addition of chitosan increases the thermal stability of cellulose, slowing down its thermal degradation (Luo et al., 2008; Pawlak & Mucha, 2003). The obtained results confirm that the interaction between the hydroxyl groups of cellulose and the

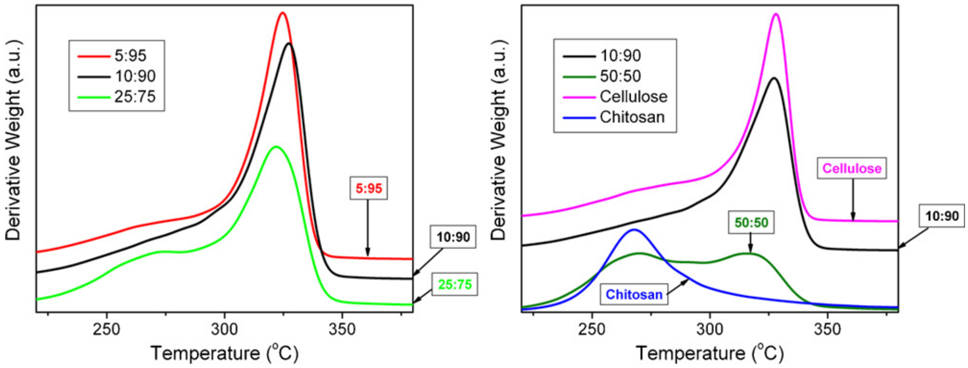

Fig. 2. Derivative plots, DTG, for chitosan (blue line), cellulose (magenta line), and chitosan–cellulose films 5/95% (w/w) (red line), 10/90% (black line), 25/75% (green line), and 50/50% (olive line). (For interpretation of the references to color in this figure legend, the reader is referred to the web version of the article.)

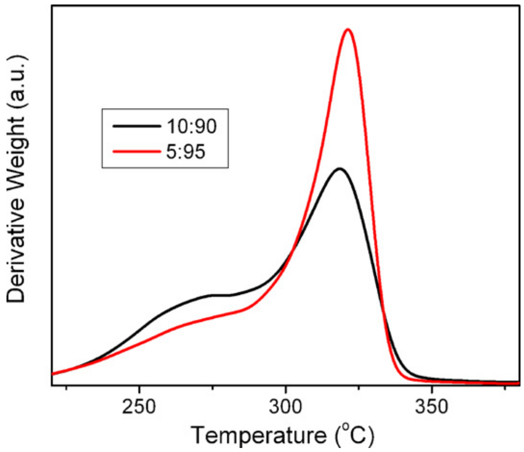

Fig. 3. Derivative plots, DTG, for physical mixture of chitosan and cellulose films of different weight percent ratios: chitosan–cellulose films 5/95% (red line), 10/90% (black line). (For interpretation of the references to color in this figure legend, the reader is referred to the web version of the article.)

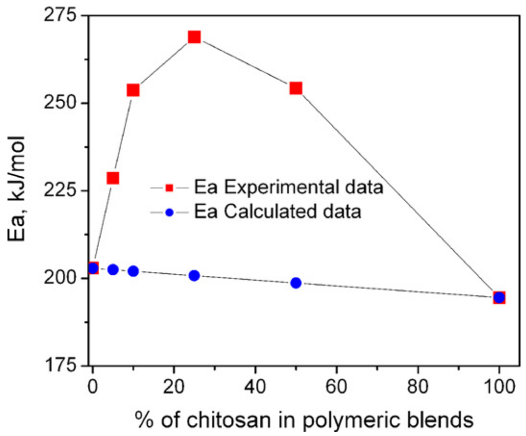

Fig. 5. The activation energy of the polymeric film component decompositions obtained from experimental data (red squares) and from calculation (blue dots). (For interpretation of the references to color in this figure legend, the reader is referred to the web version of the article.)

amino groups of chitosan established in the ionic liquid solution remained in films after the solvent removal.

The modulated temperature software developed by TA Instruments allowed the calculation of activation energy (E_a) of different processes involved in the degradation of chitosan and cellulose samples from a single experiment (Flynn, Schwenker, & Garn, 1969; MTGA, xxxx). The MTGA technique, considering the equations developed by Flynn and Wall (1966) superimposes a sinusoidal temperature modulation on the traditional underlying heating profile. This sinusoidal temperature program produces a change in the rate of weight loss. The use of discrete Fourier transformation allows kinetic parameters to be calculated on a continuous basis (Flynn et al., 1969).

The activation energy (E_a) estimated by MTGA for the degradation of cellulose film (202.9 kJ/mol) correlates very well with the $E_a \approx 170$–210 kJ/mol reported by LeVan and coworkers for thermal decomposition of cellulose in nitrogen atmosphere (LeVan, 1989). The E_a's at the onset temperature for the polymeric blends obtained from MTGA were reproducible, showing very little variation between replicate runs (±13 kJ/mol). Fig. 5 illustrates that the E_a of the chitosan film (194.5 kJ/mol) is lower than the E_a of the cellulose film (202.9 kJ/mol). The calculated E_a of the degraded polymeric blends (obtained using the weight averaged experimental E_a values of the neat polymers) (Fig. 5 – blue dots) was expected to fall between the E_a of cellulose film and the E_a of chitosan film. Also the E_a of the degraded blends is expected to decrease with the increased amount of chitosan. However, the experimental E_a of all the degraded polymeric blends (Fig. 5 – red squares) showed higher values than the E_a of both chitosan and cellulose films. These results are an indicative of enhanced stability reflecting miscibility of the two polymers. The E_a of the 25/75 chitosan/cellulose film exhibited the highest value among the polymeric films. The increased E_a for all the polymeric blends is attributed to the presence of strong interactions through hydrogen bonding between chitosan and cellulose which required higher E_a to be disrupted.

Fig. 6 shows the weight loss of cellulose, chitosan, and chitosan–cellulose blends versus time of degradation in nitrogen atmosphere at 200 °C. After 5 h of degradation, the weight loss of cellulose film was the lowest (1.3%), as compared to that of chitosan (3.4%) and chitosan–cellulose blends (2.7%, 3.2%, 4.3%, and 5.5% corresponding to 5/95%, 10/90%, 25/75%, and 50/50% blends, respectively). The weight loss of chitosan film was higher than the weight loss of the 5/95 and 10/90 wt% chitosan–cellulose blends but lower than the weight loss of the 25/75 and 50/50 wt% chitosan–cellulose films. This behavior may be explained by the presence of interactions between chitosan and cellulose through hydrogen bonding which might disrupt the crystalline structures of the polymers. The blends, being more amorphous, have the

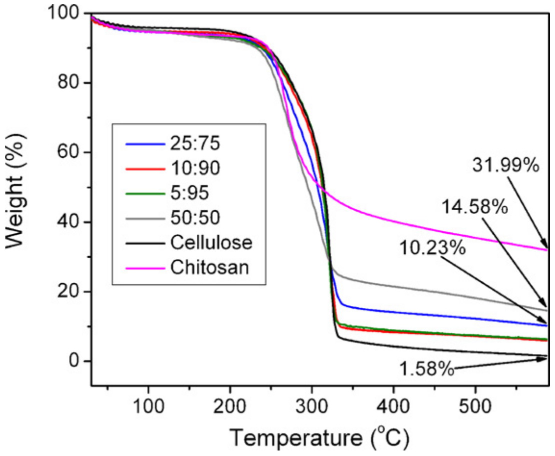

Fig. 4. Thermogravimetric plot, TG, for chitosan (magenta line), cellulose (black line), and chitosan–cellulose films 5/95% (w/w) (green line), 10/90% (red line), 25/75% (blue line), and 50/50% (gray line).

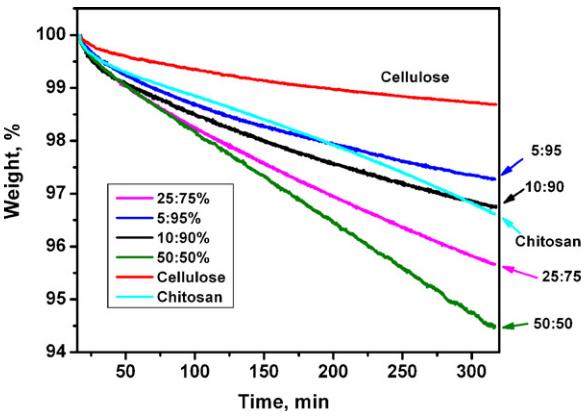

Fig. 6. Isothermal TG at 200 °C for 5 h for chitosan (cyan line), cellulose (red line), and chitosan–cellulose films 5/95% (w/w) (blue line), 10/90% (black line), 25/75% (magenta line), and 50/50% (green line). (For interpretation of the references to color in this figure legend, the reader is referred to the web version of the article.)

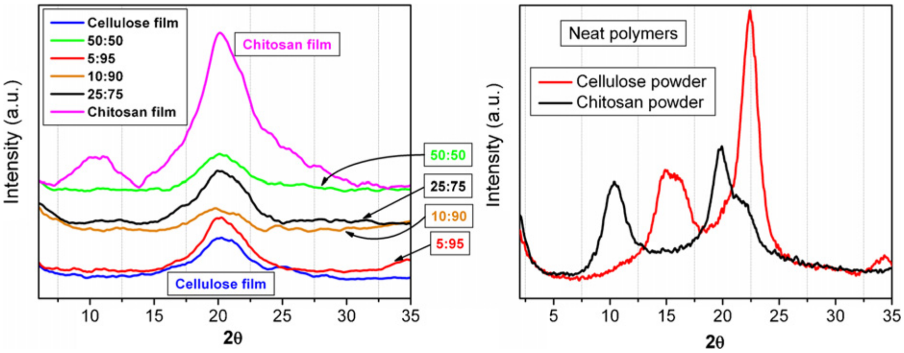

Fig. 7. XRD patterns for pure polymers and polymeric films prepared from ionic liquid solutions.

capability of retaining more water than in the cases where more crystalline regions are present. The blends containing 25 and 50 wt% chitosan are showing a higher weight loss than any of the other films because the interactions between chitosan and cellulose impede the crystallization of both components. If no interactions were present between chitosan and cellulose, one would not expect any change in the degree of crystallinity of either of the two components, and one would expect the weight loss at 200 °C for 5 h for all the polymeric blends to be proportional to chitosan content; i.e. to be between the weight loss of chitosan and that of cellulose films. Since this not the case for the polymeric blends, the isothermal data presented in Fig. 6 is further evidence for the compatibility of cellulose and chitosan through the interactions between the two polymers mentioned above.

3.3. *X-ray diffraction of polymeric films*

X-ray diffractograms of pure chitosan, pure cellulose, and chitosan–cellulose dry films prepared from ionic liquid solutions are presented in Fig. 7. The pure chitosan powder was in a crystalline state as indicated by the two main diffraction peaks at the 2θ angle of 10.7° and 19.8°. The two peaks are assigned to (0 2 0) and (1 0 0) crystallographic planes, respectively (Feng, Yu, Keao, & Zhao, 2003). These patterns, which are typical crystalline domains in this polysaccharide, are in agreement with the results reported by Nunthanid, Puttipipatkhachorn, Yamamoto, and Peck (2001) and Xu et al. (2005). After precipitating the polymer films from ionic liquid solutions, the typical diffraction pattern of native chitosan (2θ = 11.2 and 20.1°) still exists, but it exhibits smaller intensities, indicating that the native crystal structure of chitosan is reconstituted but suffers a remarkable decrease in crystallinity. The XRD pattern of pure cellulose powder shows two diffraction peaks at 2θ = 14.9 and 23.1°. The peak at 2θ angle of 23.1° originates from the cellulose crystalline plane 0 0 2 (Zhao et al., 2006). On the other hand, the diffraction pattern of the cast cellulose film exhibits a peak at 2θ = 19.9° and no peak at 14.9° which is consistent with a transformation from cellulose I to cellulose II (Hameed & Guo, 2010; Zhang, Wu, Zhang, & He, 2005). The native crystal structure of cellulose is not reconstructed, as the cast film exhibits a remarkable decrease in crystallinity, similar to the behavior of cast chitosan. This indicates that during the dissolution process, BMIMAc has broken the intra and intermolecular hydrogen bonds and disrupted the crystallinity of cellulose I.

When the two polymers were mixed at a chitosan to cellulose weight percent ratio of 5/95%, 10/90%, 25/75%, and 50/50%, only one diffraction peak with very low intensity was observed at 2θ angles around 20° (Fig. 7). All collected data were normalized to the same baseline and shifted along the intensity axis for a better comparison of final results. The presence of only one peak for the polymeric blends indicates that the chitosan structure was influenced by the addition of cellulose. The crystalline peaks of chitosan and cellulose were suppressed for all the weight percent ratios of chitosan–cellulose blends leading to a significantly lower proportion of crystalline material. Blending the two polymers makes the resulting materials more amorphous, which explains the disappearance of sharp diffraction peaks. The chitosan–cellulose blends do not show any diffraction peak at 2θ = 11.2°, behavior which could be explained by suppression of chitosan crystallization due to the formation of hydrogen bonds between chitosan and cellulose and hence miscibility between polymers (Luo et al., 2008; Xu et al., 2005).

In a diffraction process, a set of diffracted rays is obtained when a beam of X-rays is incident on a surface under an angle θ. A ray with large amplitude ($A_{\max}$) is achieved when the diffracted rays are in phase with each other (constructive interferences) while no resultant ray is formed when the diffracted rays are totally out of phase (destructive interferences). In between these two extreme situations the resultant beam may possess amplitudes comprised in between 0 and $A_{\max}$ (Moore & Reynolds, 1997; Stefanescu, Daly, & Negulescu, 2008). This explains why there is no trend for the intensity of crystalline peak of the polymeric blends with the increase of chitosan content. The thickness of the films could not be kept the same and as a result rays with different amplitude were obtained due to the presence of constructive or destructive interferences.

3.4. *SEM experiments of polymeric films*

The SEM micrographs obtained from freeze dried chitosan and/or cellulose films are presented in Figs. 8–10. The thickness of the films varied between 1 mm and 1.2 mm. The films were prepared by shear spreading a polymer-solution on a Teflon mold followed by polymer precipitation in methanol and water. Prior to SEM analysis the dried films were fractured following an axis perpendicular to the spreading direction. The fracture surface XY plane is defined in image ***a*** (Fig. 8). Image ***b*** represents a magnified version of the area delimited with a dashed line in image ***a***.

The SEM of pure chitosan and pure cellulose films are presented in Fig. 8. In the top of Fig. 8 it can be easily observed that overall the precipitated chitosan film has a very porous and disorganized structure, in which the domains have no particular orientation. In image ***a*** it is apparent that the density of striations is higher towards the middle-bottom part of the film, along the thickness axis *X*, rather than at the top surface. An explanation could be related to the presence of solvent-rich and polymer-rich domains along the thickness of the film. If that was the case, the solvent-rich domains would be expected to induce a higher density of striations in the precipitated polymer, upon immersion in methanol and water. In image ***b*** it is apparent that the main structure of large striations that are visible in ***a***, is interpenetrated by a secondary structure of smaller

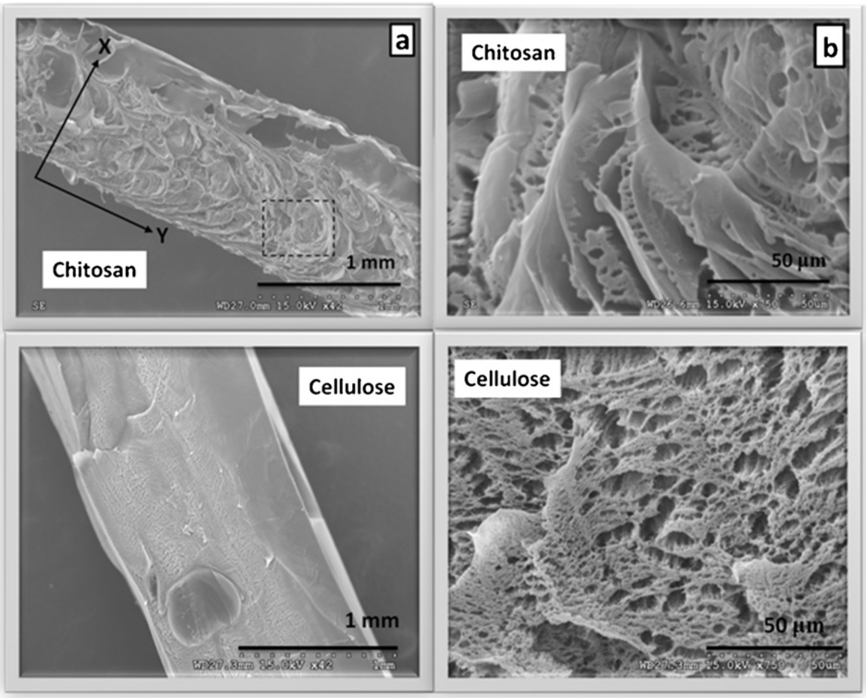

Fig. 8. SEM micrographs of freeze dried chitosan film and cellulose film prepared through shear spreading (cross-section).

striations. Overall, it is hard to quantify the porosity of the film since various individual features exhibit different dimensions.

In the case of cellulose film (bottom of Fig. 8) a well-organized fiber-like network oriented along the spreading direction can be observed. The fibers seem to be parallel to each other but have a random distribution. Voids ranging from 1.9 μm to 13.5 μm are present throughout the fiber-like structure. These voids are the result of the extraction of the solvent from the cellulose ionic liquid solutions during the polymer precipitation process. The freeze-drying technique applied to the wet films was performed to prevent the collapsing of the polymeric films after the polymers were precipitated in water.

The morphology of the polymeric blends is quite different from that of pure chitosan and depends on the chitosan–cellulose weight percent ratio. For the samples with a 5/95% chitosan–cellulose, the cross-section structure resembles that of cellulose with a fiber-like network oriented along the spreading direction and voids varying from 1.9 μm to 10.4 μm (Fig. 9). These voids may be considered as “cracks” with no particular order. The same structure can be observed for the 10/90% chitosan–cellulose blend with an

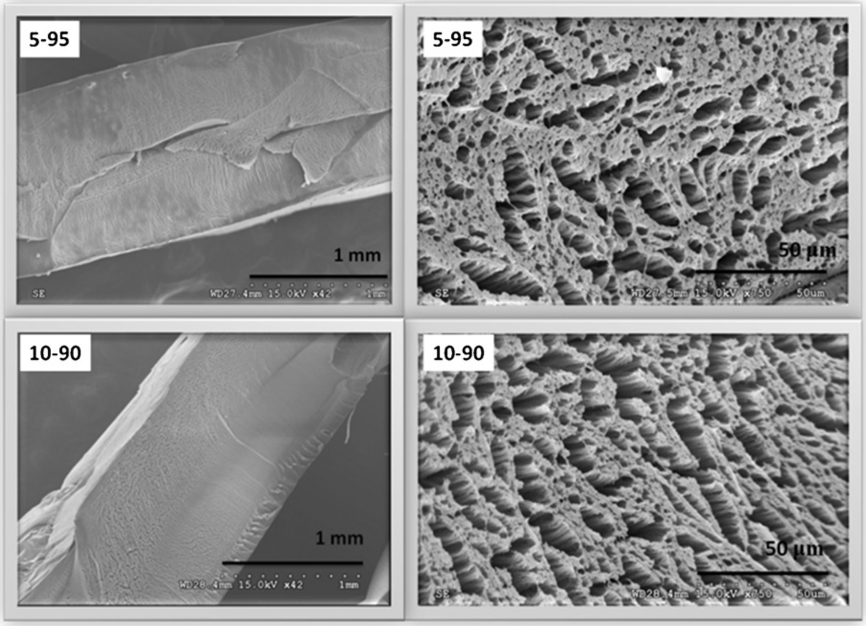

Fig. 9. SEM micrographs of freeze dried chitosan/cellulose (5/95% and 10/90%) blend prepared through shear spreading (cross-section).

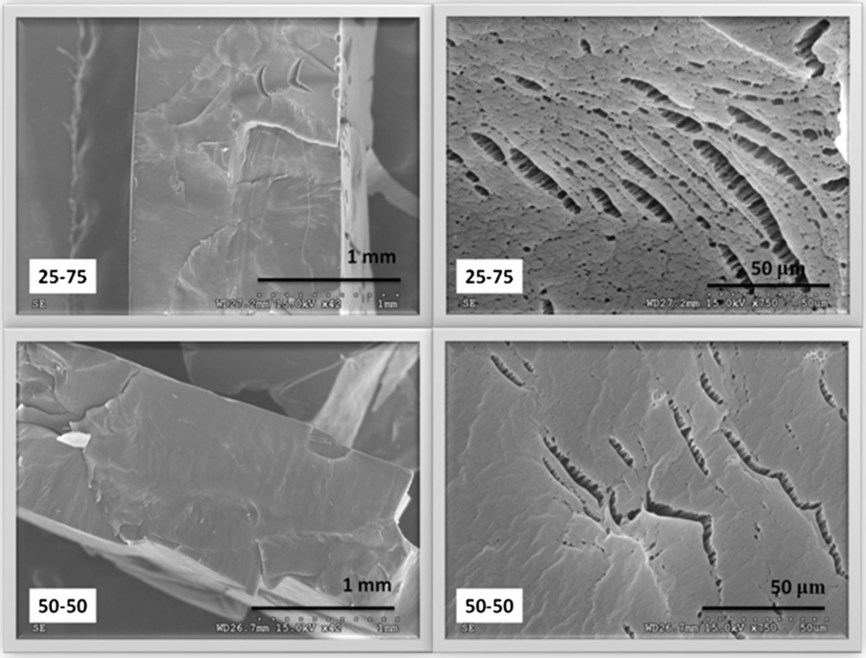

Fig. 10. SEM micrographs of freeze dried chitosan/cellulose (25/75% and 50/50%) blend prepared through shear spreading (cross-section).

ordered fiber-like structure and uniformly distributed voids ranging from 1.9 μm to 10.4 μm (Fig. 9). However, the fiber-like network seems to be more organized than in the case of cellulose or 5/95% chitosan–cellulose blend with the "cracks" being mostly parallel to each other. When the amount of chitosan in the polymeric blends is increased to 25 wt% (Fig. 10), the cross-section of the corresponding film shows a more compact structure with fewer parallel voids than in the case of the blends with less than 25 wt% chitosan in their composition. The "cracks" are also smaller in size (8.33 μm). Fig. 10 also illustrates the SEM micrographs at different magnifications of the 50/50% chitosan–cellulose blends. The cross-section of the films looks more like a smooth surface with few "cracks" of about 4.16 μm. By looking at the voids it can be seen that the fiber-like network is present for this composition of blends (50/50%) as well. A homogeneous structure with no phase separation of the two polymers, cellulose and chitosan, was observed for all of the blends. Thus the SEM data is consistent with miscibility between chitosan and cellulose in the solid state.

4. Conclusions

Blends of chitosan and cellulose were successfully prepared using BMIMAc as a solvent. Films prepared from the polymeric solutions were investigated by means of FT-IR, TGA, X-ray diffraction and SEM measurements. The shifting of the bands corresponding to –NH and C=O groups of chitosan (FT-IR), the absence of the diffraction peaks at $2\theta = 10.7$ and 14.9° (XRD), the increased E_a for all the polymeric blends (MTGA), and the presence of a homogeneous structure with no apparent phase separation of the two polymers (SEM) serve as evidence for the miscibility between chitosan and cellulose in the solid state.

Acknowledgements

Partial financial support is acknowledged from the USDA multistate Hatch program S-1026 LSU Project 93816 (LSU AgCenter).

References

Almeida, E. V. R., Frollini, E., Castellan, A., & Coma, V. (2010). Chitosan, sisal cellulose, and biocomposite chitosan/sisal cellulose films prepared from thiourea/NaOH aqueous solution. *Carbohydrate Polymers*, *80*, 655–664.

Feng, T., Yu, L., Keao, H., & Zhao, B. (2003). The depolymerization mechanism of chitosan by hydrogen peroxide. *Journal of Materials Science*, *38*, 4709–4712.

Flores-Ramirez, N., Elizalde-Pena, E. A., Vasquez-Garcia, S. R., Gonzalez-Hernandez, J., Martinez-Ruvalcaba, A. M., Sanchez, I. C., et al. (2005). Characterization and degradation of functionalized chitosan with glycidyl methacrylate. *Journal of Biomaterials Science-Polymer Edition*, *16*, 473–488.

Flynn, J. H., & Wall, L. A. (1966). General treatment of the thermogravimetry of polymers. *Polymer Letter*, *19*, 323.

Flynn, J. H., Schwenker, J., & Garn, P. D. (1969). *Thermal analysis*. New York: Academic Press. (p. 1111).

Goosen, M. F. A. (1997). *Applications of chitin and chitosan*. CRC Press LLC.

Hameed, N., & Guo, Q. (2010). Blend films of natural wool and cellulose prepared from an ionic liquid. *Cellulose*, *17*, 803–813.

LeVan, S. L. (1989). Thermal degradation. In A. P. Schniewind (Ed.), *Concise encyclopedia of wood & wood-based materials*. New York: Pergamon Press.

Liu, C. F., Sun, R. C., Zhang, A. P., Qin, M. H., Ren, J. L., & Wang, X. A. (2007). Preparation and characterization of phthalated cellulose derivatives in room-temperature ionic liquid without catalysts. *Journal of Agricultural and Food Chemistry*, *55*, 2399–2406.

Liu, C. F., Sun, R. C., Zhang, A. P., & Ren, J. L. (2007). Preparation of sugarcane bagasse cellulosic phthalate using an ionic liquid as reaction medium. *Carbohydrate Polymers*, *68*, 17–25.

Luo, K., Yin, J., Khutoryanskaya, O. V., & Khutoryanskiy, V. V. (2008). Mucoadhesive and elastic films based on blends of chitosan and hydroxyethylcellulose. *Macromolecular Bioscience*, *8*, 184–192.

Miya, M., Iwamoto, R., Yoshikawa, S., & Mima, S. (1980). IR Spectroscopic determination of CONH content in highly deacylated chitosan. *International Journal of Biological Macromolecules*, *2*, 323–324.

Moore, D. M., & Reynolds, C. R., Jr. (1997). *X-ray diffraction and the identification and analysis of clay minerals*. New York: Oxford University Press.

MTGA. (xxxx). Application Brief TA-237 Modulated Thermogravimetric Analysis: A new approach for obtaining kinetic parameters. TA Instruments. http://www.tainstruments.com/pdf/literature/TA237.pdf.

Muzzarelli, R. A. A. (1973). *Natural chelating polymers*. Toronto: Pergamon of Canada Ltd.

Nakajima, A., & Shinoda, K. (1977). Permeation properties of glycol chitosan–mucopolysaccharide complex membranes. *Journal of Applied Polymer Science*, *21*, 1249–1255.

Nunthanid, J., Puttipipatkhachorn, S., Yamamoto, K., & Peck, G. E. (2001). Physical properties and molecular behavior of chitosan films. *Drug Development and Industrial Pharmacy*, *27*, 143–157.

Pawlak, A., & Mucha, M. (2003). Thermogravimetric and FTIR studies of chitosan blends. *Thermochimica Acta*, *396*, 153–166.

Phisalaphong, M., & Jatupaiboon, N. (2008). Biosynthesis and characterization of bacteria cellulose–chitosan film. *Carbohydrate Polymers*, *74*, 482–488.

Rao, V., & Johns, J. (2008). Thermal behavior of chitosan/natural rubber latex blends. TG and DSC analysus. *Journal of Thermal Analysis and Calorimetry*, *92*, 801–806.

Rha, C., Rodriguez-Sanchez, D., & Kienzle-Sterzer, C. (1984). In R. R. Colwell, E. R. Pariser, & A. J. Sinskey (Eds.), *Biotechnology of marine polysaccharides* (pp. 283–311). Washington: Hemisphere Publishing Corp.

Rogers, R. D., & Seddon, K. R. (2003). CHEMISTRY: Ionic liquids-solvents of the future? *Science*, *302*, 792–793.

Shigehiro, H., Kenji, T., Masahiro, H., & Noriaki, M. (1980). Permeability properties of gels and membranes derived from chitosan. *Journal of Biomedical Materials Research*, *14*, 477–485.

Shih, C. M., Shieh, Y. T., & Twu, Y. K. (2009). Preparation and characterization of cellulose/chitosan blend films. *Carbohydrate Polymers*, *78*, 169–174.

Simmons, T. J., Lee, S. H., Miao, J., Miyauchi, M., Park, T. J., Bale, S. S., et al. (2010). *Preparation of synthetic wood composites using ionic liquids*. Wood Science and Technology.

Stefanescu, E. A., Daly, W. H., & Negulescu, I. I. (2008). Hybrid polymer/clay nanocomposites: Effect of clay size on the structure of multilayered films. *Macromolecular Materials and Engineering*, *293*, 651–656.

Stefanescu, C., Daly, W. H., & Negulescu, I. I. (2009a). 1-Butyl-3-methylimidazolium acetate as a solvent media for functionalization of chitosan. *Polymer Preprints*, *50*, 143–144.

Stefanescu, C., Daly, W. H., & Negulescu, I. I. (2009b). Nucleophilic reactivity of chitosan in ionic liquids promoted by tert-amines. *Polymer Preprints*, *50*, 551–552.

Sun, X., Peng, B., Ji, Y., Chen, J., & Li, D. (2009). Chitosan(chitin)/cellulose composite biosorbents prepared using ionic liquid for heavy metal ions adsorption. *AlChe Journal*, *55*, 2062–2069.

Swatloski, R. P., Spear, S. K., Holbrey, J. D., & Rogers, R. D. (2002). Dissolution of cellulose with ionic liquids. *Journal of the American Chemical Society*, *124*, 4974–4975.

Wu, A. C. M., Bough, W. A., Holmes, M. R., & Perkins, B. E. (1978). Influence of manufacturing variables on the characteristics and effectiveness of chitosan products. III. Coagulation of cheese whey solids. *Biotechnology and Bioengineering*, *20*, 1957–1966.

Wu, Y.-B., Yu, S.-H., Mi, F.-L., Wu, C.-W., Shyu, S.-S., Peng, C.-K., et al. (2004). Preparation and characterization on mechanical and antibacterial properties of chitsoan/cellulose blends. *Carbohydrate Polymers*, *57*, 435–440.

Xiao, W., Chen, Q., Wu, Y., & Wu, T. (2011). Dissolution and blending of chitosan using 1,3-dimethylimidazolium chloride and 1-H-3-methylimidazolium chloride binary ionic liquid solvent. *Carbohydrate Polymers*, *83*, 233–238.

Xu, Y. X., Kim, K. M., Hanna, M. A., & Nag, D. (2005). Chitosan–starch composite film: Preparation and characterization. *Industrial Crops and Products*, *21*, 185–192.

Yin, J., Luo, K., Cheng, X., & Khutoryanskiy, V. V. (2006). Miscibility studies of the blends of chitosan with some cellulose ethers. *Carbohydrate Polymers*, *63*, 238–244.

Zhang, H., Wu, J., Zhang, J., & He, J. (2005). 1-Allyl-3-methylimidazolium chloride room temperature ionic liquid: A new and powerful nonderivatizing solvent for cellulose. *Macromolecules*, *38*, 8272–8277.

Zhao, H., Kwak, J. H., Wang, Y., Franz, J. A., White, J. M., & Holladay, J. E. (2006). Effects of crystallinity on dilute acid hydrolysis of cellulose by cellulose ball-milling study. *Energy and Fuels*, *20*, 807–811.

Zhao, Q., Yam, R. C. M., Zhang, B., Yang, Y., Cheng, X., & Li, R. K. Y. (2009). Novel all-cellulose ecocomposites prepared in ionic liquids. *Cellulose*, *16*, 217–226.

Zhu, S. D., Wu, Y. X., Chen, Q. M., Yu, Z. N., Wang, C. W., Jin, S. W., et al. (2006). Dissolution of cellulose with ionic liquids and its application: A mini-review. *Green Chemistry*, *8*, 325–327.